International Journal of Advanced Technology and Innovative Research

ISSN 2348–2370
Vol.09,Issue.07,
June-2017,
Pages:1060-1065

www.ijatir.org

A New Topology of Phase Shift Operated Interleaved DC-DC Converter Interconnected with Grid

SHEIK BABJI[1], S. S. SRIRAM[2]

[1]PG Scholar, Dept of EEE, BVCITS, Batlapalem, Amalapuram, AP, India.

[2]Assistant Professor, Dept of EEE, BVCITS, Batlapalem, Amalapuram, AP, India.

Abstract: In this era of rapid industrialization, renewable energy is progressively more valued and utilized worldwide owing to energy shortage and environmental contamination. The output voltage obtained from the renewable energy systems is incredibly low. So, for several renewable energy applications like photo voltaic systems, Fuel Cells, solar power generation, high step-up dc to dc converters have been used for such systems to remodel the low voltage energy from the Hybrid resources into high voltage using a step-up converter. Here we present a new grid connected power system using Alternative phase shift based PWM for DC-DC converter for Dc power generation system by integrating alternating phase shift (APS) control and the conventional interleaving PWM control. This integration give the following advantages 1) APS control is helpful to decrease the voltage stress on switches in light load and 2) the conventional interleaving control is valuable to keep better system performance in heavy load. For interchanging the modes between APS and conventional PWM control, a boundary condition has been derived. This converter is operated in grid system application connected to three phase voltage source converters to feed the load and grid. In this paper, we are simulating Grid connected DC-DC converter and validate the results.

Keywords: Boost Converter, Interleaved, Voltage Multiplier.

I. INTRODUCTION

With increasing anxiety about energy and atmosphere, it is essential to discover the renewable energy such assolar, wind power, fuel cell, etc. Fuel cell is one of hopeful choices due to its higher power density, advantages of zero emission, little noise, and simply modularized for electric vehicles, convenient power sources, distributed generation systems, etc[1]. The grid associated power system based on fuel cell technology is shown in Fig. 1. For a distinctive 10-kW proton exchange membrane fuel cell, the output voltage is from 65 to 107 V. Nevertheless, the input voltage for the three phase dc/ac converter (inverter) needs to be roughly 700 V, the voltage increase of the dc/dc converter connecting fuel cell and the dc/ac converter will be around 6 to 11 V. Therefore a high step-up dc/dc converter is required for the system as shown in Fig. 1. The dc/dc converter will produce a high frequency input current ripple, and tries to reduce the life time of the fuel cell stack [2]–[4]. Adding together, the hydrogen energy utilization reduces with growing the current ripple of the fuel cell stack [5]. Hence, the dc/dc converter should have high step-up ratio with minimum input current ripple for the system as shown in Fig. 1.

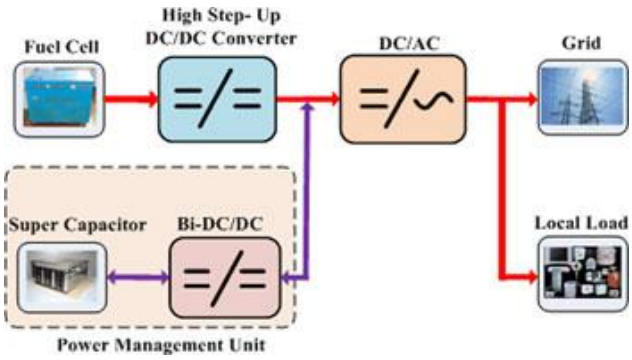

Fig. 1 Grid-connected power system based on fuel cell.

High step-up ratio can be received by integrating traditional boost converter with coupled inductors [7]–[9], switched inductors [6], high-frequency transformer [10], or switched capacitor [11]. These can attain high step-up ratio with more efficiency, low electromagnetic interference and low-voltage stress. Either a passive filter [5] or an active filter [5] can be used to decrease output current ripple or the dc/dc converter input current ripple, nevertheless, this will enlarge the difficulty of the system. In detail, interleaving the dc/dc converter can decrease the input current ripple of the dc/dc converter [6]. An interleaved boost converter with voltage multiplier was projected in [13]. This system voltage gain was amplified up to (M +1) times (M-number of the voltage multiplier) of the traditional boost converter with the identical duty cycle D and minor voltage stress. Further, it has lesser input current and output voltage ripples in comparison to the traditional boost converter. The interleaving DC-DC boost converter with voltage multipliers is shown in Fig2. The DC-DC boost converter shown in Fig2 can attain small voltage stress in the power devices, which raises the conversion efficiency. Nevertheless, this is only correct in heavy load once the voltage stress of the power devices mayenlarge when it works in discontinuous conduction mode (DCM) [7], this occurs while fuel cell barely supplies a light local load as shown in Fig. 1.

In this situation, superior voltage power devices require to be used, and consequently its cost and power loss will be improved. The authors proposed an Alternative phase shift based PWM for DC-DC converter for DC power generation system, to overcome the difficulty when the converter operates in light load [7][8].

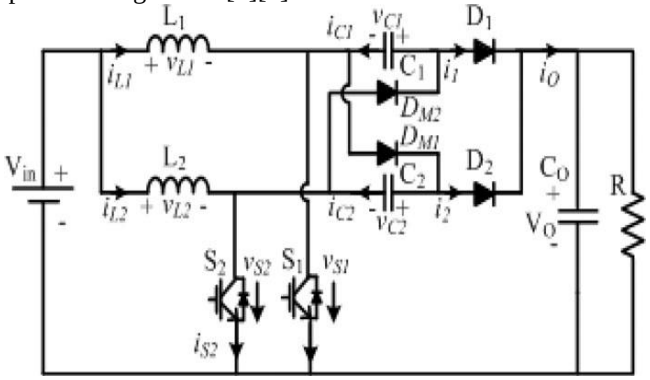

Fig 2. Structure of two-phase interleaved boost converter with voltage multiplier.

This manuscript presents A new grid connected power system using Alternative phase shift based PWM for DC-DC converter for DC power generation system by integrating alternating phase shift (APS) control and the conventional interleaving PWM control. For interchanging the modes between APS and conventional PWM control, a boundary condition has been derived. This converter is operated in grid system application connected to three phase voltage source converter to feed the load and grid. The proposed system is designed in MATLAB/SIMULINK.

II. PROPOSED SYSTEM OPERATION

It is assumed that all components in the converter are ideal, both capacitor C1 and C2 are large enough, and duty cycle is less than 0.5. The operation of a switching cycle of the converter can be divided into six stages at boundary condition which the voltage stress on switch will be larger than half of the output voltage with traditional interleaving control, as shown in Fig. 3. Typical theoretical waveforms at boundary condition are shown in Fig. 4.

A. First Stage (t0, t1): At the moment of t0, both switch S1 and S2 are off, the energy stored in the inductor L2 and capacitor C2 in previous stage are transferred to the output capacitor CO through D2 as shown in Fig. 3(a). The voltage stress on switch S1 is the input voltage Vin, and the voltage stress on switch S2 is (VO −VC2), where VO is the output voltage and VC2 is the voltage of capacitor C2.

B. Second Stage (t1, t2): At the moment of t1, the switch S1 is turned ON, the inductor L1 starts to store energy from zero as shown in Fig. 3(b). In the meantime, if (VC1 +VC2) < VO , where VC1 is the capacitor C1 voltage, the diode D2 will be turned OFF and the diode DM2 will be turned ON; therefore, the energy in the inductor L2 will be transferred to the capacitor C1 . If there is enough energy in the inductor L2, VC1 will be charged to the following state: VC1 + VC2 ≥ VO. Then, the diode D2 will be turned ON again, which is shown in Fig. 5. If there is not enough energy to charge VC1 to (VO − VC2), then it will come to the Third Stage as shown in Fig. 3(c). If the energy in the inductor L2 is just discharged to zero and VC1 + VC2 = VO at the end of the stage, then we say that the circuit operates in the boundary condition state. During the stage, the voltage stress-on switch S2 is VC1.

C. Third Stage (t2, t3): At the moment of t2, the current in the inductor L2 just falls to zero, all the diodes are in off state and the inductor L1 is in charging state until the switch S1 is turned OFF at the moment of t3. The voltage stress on switch S2 is Vin. At the end of this stage, the current in the inductor L1 comes to the peak value IL1P, and

$$I_{L1P} = \frac{V_{\text{in}} D_m T_S}{L} \tag{1}$$

Where Vin is the input voltage, L is the inductance of L1 and L2, Dm is the duty cycle at boundary condition, and TS is the switching period.

D. Fourth Stage (t3, t4): At the moment of t3, switch S1 and S2 are in off state, the energy in the inductor L1 and the capacitor C1 will be transferred to the output capacitor CO through the diode D1, which is similar to First Stage. In this stage, the voltage stress on switch S1 is (VO − VC1), and the voltage stress on switch S2 is Vin. At the end of this stage, the current in the inductor L1 decreases to be IL1M

$$I_{L1M} = I_{L1P} - \frac{V_O - V_{C1} - V_{\text{in}}}{L}(0.5 - D_m)T_S. \tag{2}$$

E. Fifth Stage (t4, t5): At the moment of t4, the switch S2 is turned ON and the inductor L2 starts to store energy. This stage is similar to the Second Stage. In this stage, the voltage stress on switch S1 is VC2. At the end of this stage, the current in the inductor L1 decreases to zero from IL1M. And thus

$$I_{L1M} - \frac{V_{C2} - V_{\text{in}}}{L}(D_2 - 0.5 + D_m)T_S = 0 \tag{3}$$

Where D2 is the duty cycle as shown in Fig. 4.

F. Sixth Stage (t5, t6): At the moment of t5, the current in the inductor L1 decreases to zero. All the diodes are in off state and the inductor L2 is in charging state until the stage comes to the end at the moment t6. A new switching period will begin with the next First Stage. From the aforementioned analysis, the voltage sum of capacitor C1 and C2 will be VO at boundary condition. If it is less than VO, the voltage stress on switch S1 and S2 will be larger than VO /2, because the voltage stress on switch S1 is (VO − VC1) during the Fourth Stage and the voltage stress on switch S2 is (VO − VC2) during the First Stage. The average value of the output current Io is equal to the dc component of the load current VO/R, then

$$\frac{V_O}{R} = \frac{1}{T_S}\int_0^{T_S} i_O\,dt = \frac{1}{T_S}\int_0^{T_S} (i_1 + i_2)dt$$
$$= \frac{1}{T_S}\int_0^{T_S} i_1\,dt + \frac{1}{T_S}\int_0^{T_S} i_2\,dt. \tag{4}$$

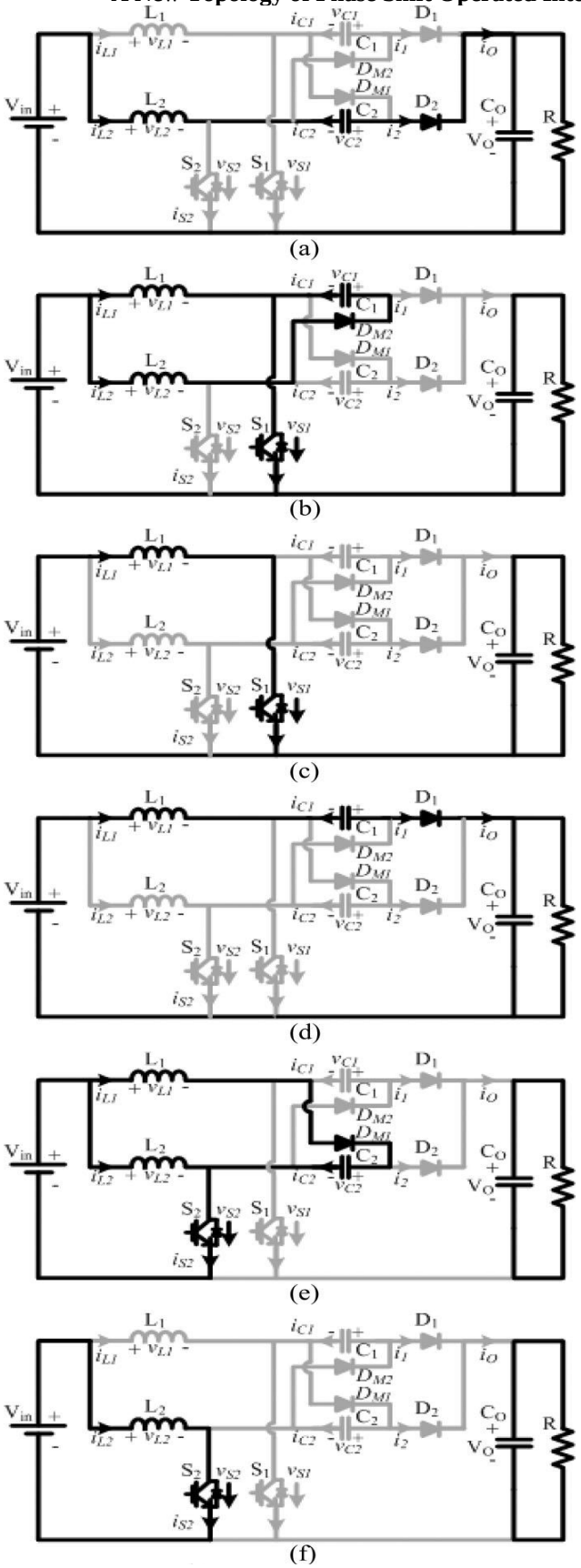

Fig.3.Stages at boundary condition (a) First stage (t0, t1), (b) second stage (t1, t2), (c) third stage (t2, t3), (d) fourth stage (t3, t4), (e) fifth stage (t4, t5), (f) sixth stage (t5 , t6).

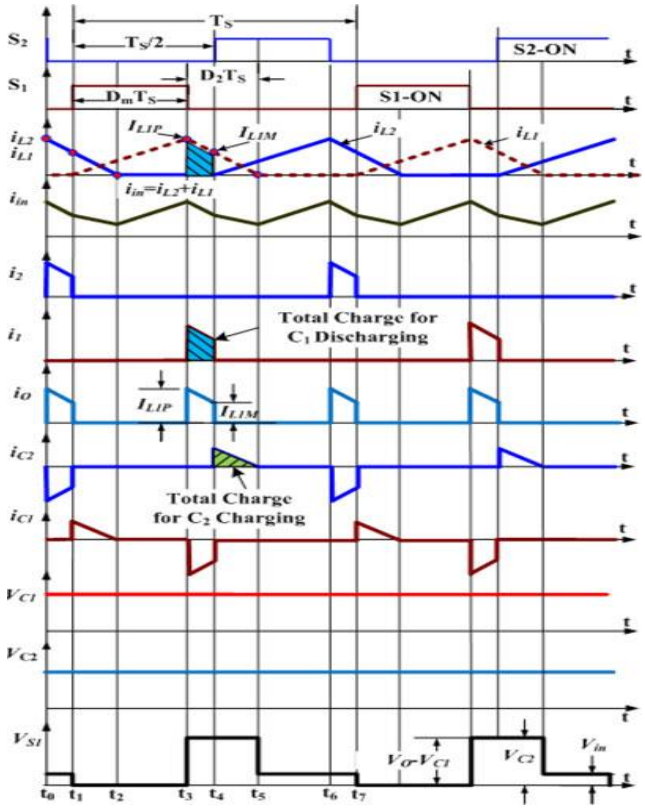

Fig4. Main theoretical waveforms at boundary condition.

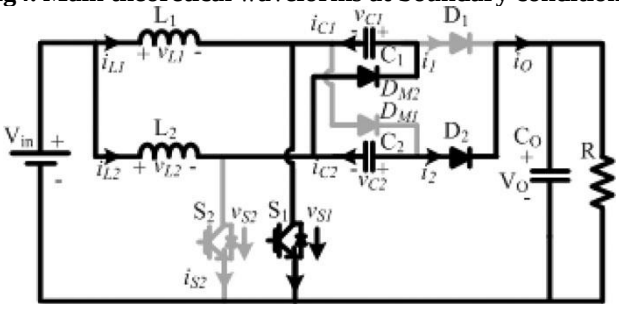

Fig 5. One stage above boundary condition.

Considering the same parameters of the circuit in two phases as shown in Fig. 2, therefore

$$\frac{1}{T_S}\int_0^{Ts} i_1 dt = \frac{1}{T_S}\int_0^{Ts} i_2 dt. \tag{5}$$

By combining (4) and (5), it is derived

$$\frac{V_O}{R} = \frac{2}{T_S}\int_0^{Ts} i_1 dt = \frac{2}{T_S}\int_{t3}^{t4} i_1 dt$$

$$= \frac{2}{T_S}\cdot\left[\frac{1}{2}(I_{L1P}+I_{L1M})(0.5-D_m)T_S\right]$$

$$= (I_{L1P}+I_{L1M})(0.5-D_m) \tag{6}$$

Where R is the load.

At the boundary condition, the diodeD2 (D1) approaches the conduction state during the Second Stage (Fifth Stage), which is shown in Fig5. The following equation can be obtained

$$V_{C1}+V_{C2}=V_O. \tag{7}$$

Considering both capacitors C1 and C2 are large enough, average voltage of the capacitor will keep equal. Otherwise, the converter will not operate at boundary condition, therefore

$$V_{C1} = V_{C2} = \frac{1}{2}V_O. \quad (8)$$

By substituting (1) and (8) into (2), the current IL1M can be derived

$$I_{L1M} = \frac{V_{\text{in}} - V_O/2 + V_O \cdot D_m}{2L} T_S. \quad (9)$$

As shown in Fig. 4, the total discharge of capacitor C1 between t3 and t4 is

$$Q_{C1} = \int_{t_3}^{t_4} i_{L1}dt = \frac{1}{2}(I_{L1P} + I_{L1M})(0.5 - D_m)T_S. \quad (10)$$

The total charge of capacitor C2 between t4 and t5 is

$$Q_{C2} = \int_{t_4}^{t_5} i_{L1}dt = \frac{1}{2}I_{L1M}(D_2 - 0.5 + D_m)T_S. \quad (11)$$

According to the previous analysis, the total discharge of C1 is equal to the total charge of capacitor C2 at boundary condition. Therefore, there will be

$$Q_{C1} = Q_{C2}. \quad (12)$$

By combining (10), (11), and (12), the following can be derived

$$D_2 = (0.5 - D_m)\left(\frac{I_{L1P}}{I_{L1M}} + 2\right). \quad (13)$$

By combining (3) and (6) and then substituting (1), (9), and (13) into them, the boundary condition can be derived as

$$\begin{cases} K = K\text{crit} = \dfrac{n-2}{2n(n-\sqrt{2})^2} & (a) \\ D_m = \dfrac{n-2}{2(n-\sqrt{2})} & (b) \end{cases} \quad (14)$$

Where n is the voltage gain of the converter (n = VO /Vin), and K is the parameters of the circuit and K = 2L/(R × TS). The boundary constraint with traditional interleaving control decided by (14) is shown in Fig. 6. The constraint includes two parts: duty cycle D and the circuit parameters K = 2L/(R ×TS).

As the switching period TS and the input inductor L are designed at nominal operation in continuous conduction mode(CCM), the constraint is determined by duty cycle D and the load R. The reason why there are two parts in the boundary constraint is that the duty cycle D varies with the load when the converter operates in DCM. For a given application, the voltage gain of the dc/dc converter is determined. And then, the minimum duty cycle that can maintain low-voltage stress in main power devices with traditional interleaving control will be given by (14)-(b) and as shown in Fig. 6(a). At the same minimum duty cycle, the converter operates at boundary condition when the circuit parameters K = 2L/(R×TS) satisfy (14)-(a)and as shown in Fig. 6(b). When the converter operates above the boundary condition, the circuit parameters are in Zone of Fig. 6(b), i.e.,K >Kcrit, the converter could achieve halved voltage stress on switches with traditional interleaving control with the duty cycle above the solid red line as shown in Fig. 6(a). When decreasing the load to the solid red line at boundary condition in Fig. 6(b), i.e., K = Kcrit, the duty cycle of the converter will be decreased to the solid red line in Fig. 6(a). When decreasing the load further in Zone B in Fig. 6(b), i.e., K <Kcrit , the duty cycle will be decreased further to be smaller than the minimum duty cycle that maintains low-voltage stress on switches with traditional interleaving control. Then, the APS control should be used to achieve halved voltage stress on switches in Zone B [17], [18]. When the circuit parameters K = 2L/(R ×TS) are below the solid red line from point a to point b at different voltage gain as shown in Fig. 6(b), the duty cycle will be decreased further to be less than the solid red line from Dm1 = 0.443 to Dm2 = 0.456as shown in Fig. 6(a), and then the voltage stress on switches will be increased at this load. In order to achieve the halved voltage stress on switches at this load, APS control is needed.

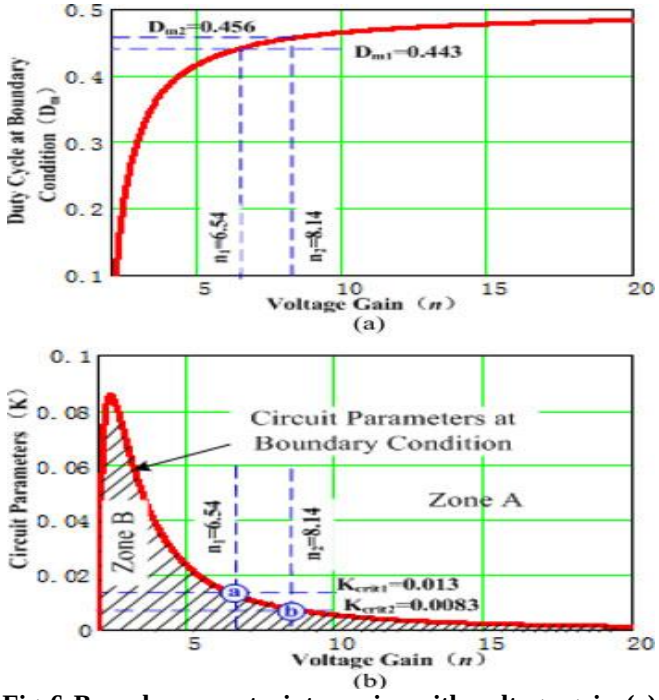

Fig 6 Boundary constraints varies with voltage gain (a) Duty cycle at boundary condition varies with voltage gain (b) circuit parameters at boundary condition varies with voltage gain.

III. SIMULATION RESULTS

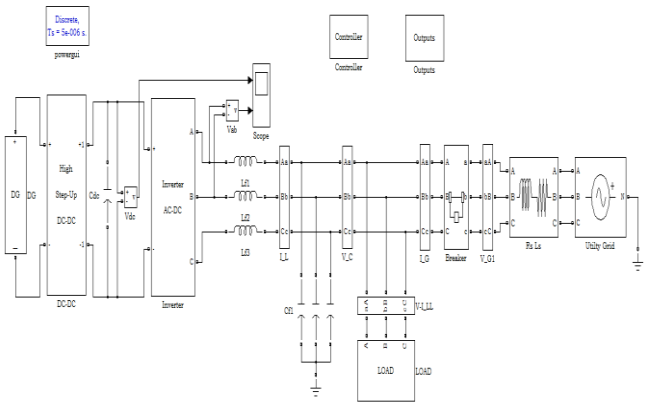

Fig7. Simulation diagram of proposed DC–DC converter connected to load and grid.

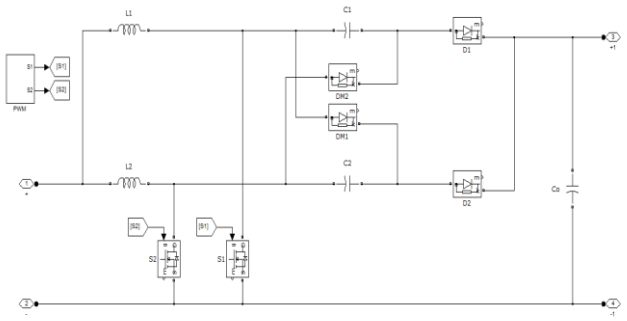

Fig 8. Simulation model of proposed DC-DC converter.

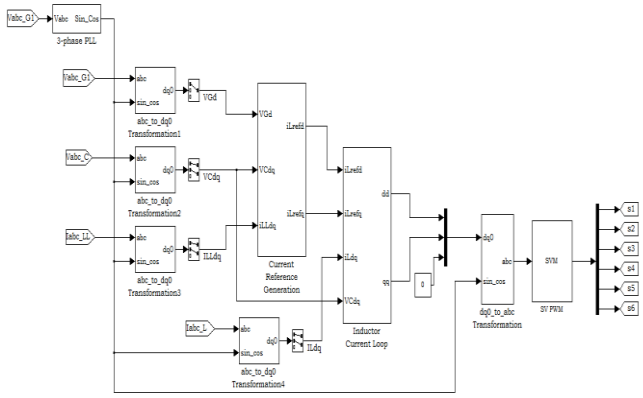

Fig 9. Simulation diagram of alternating phase shift (APS) control and traditional interleaving PWM control.

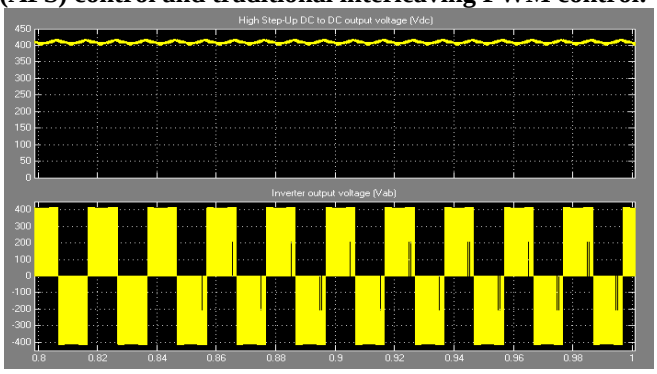

Fig 10. High step-up DC-DC converter output voltage and inverter output voltage.

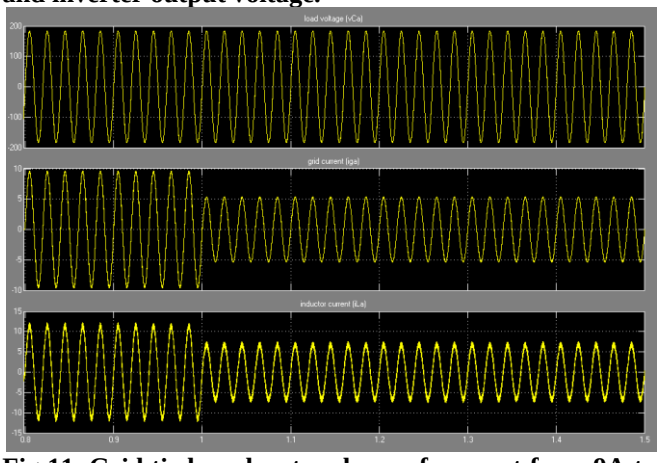

Fig 11. Grid tied mode: step down of current from 9A to 5A i) load voltage ii) grid current and iii) inductor current.

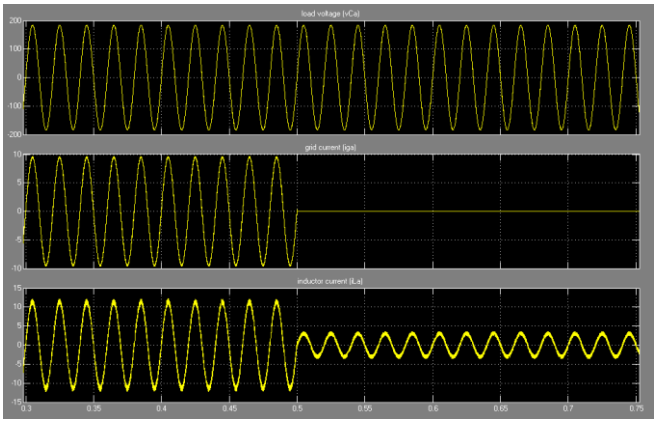

Fig 12. Change from grid tied mode to islanding mode i) load voltage ii) grid current and iii) inductor current.

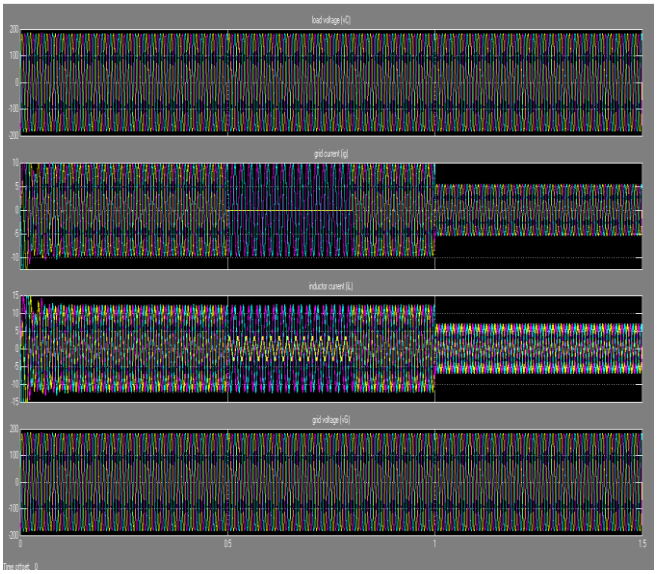

Fig 13. Three phase simulated waveforms i) load voltage ii) grid voltage iii) inductor current and iv) grid currents.

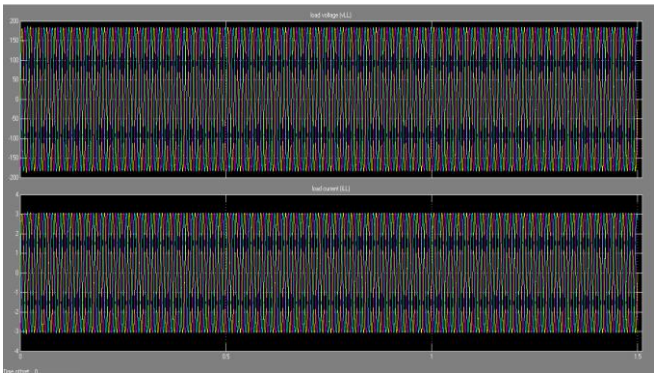

Fig 14. Three phase load voltages and load currents.

IV. CONCLUSION

In the paper the boundary condition for the operation of converter is derived by mathematical analysis. The boundary condition classifies the operating states into two zones, i.e., Zone A and Zone B. The traditional interleaving control is used in Zone A while APS control is used in Zone B. And the swapping function is achieved by a logic unit. With the

proposed control scheme, the converter can achieve low voltage stress on switches in all power range of the load, which is verified by simulation results.

V. REFERENCES

[1] N. Sammes, Fuel Cell Technology: Reaching Towards Commercialization. London, U.K.: Springer-Verlag, 2006.
[2] G. Fontes, C. Turpin, S. Astier, and T. A. Meynard, "Interactions between fuel cells and power converters: Influence of current harmonics on a fuelcell stack," IEEE Trans. Power Electron., vol. 22, no. 2, pp. 670–678, Mar.2007.
[3] P. Thounthong, B. Davat, S. Rael, and P. Sethakul, "Fuel starvation," IEEE Ind. Appl. Mag., vol. 15, no. 4, pp. 52–59, Jul./Aug. 2009.
[4] S.Wang, Y. Kenarangui, and B. Fahimi, "Impact of boost converter switching frequency on optimal operation of fuel cell systems," in Proc. IEEE Vehicle Power Propulsion Conf., 2006, pp. 1–5.
[5] S. K. Mazumder, R. K. Burra, and K. Acharya, "A ripple-mitigating and energy-efficient fuel cell power-conditioning system," IEEE Trans. Power Electron., vol. 22, no. 4, pp. 1437–1452, Jul. 2007.
[6] B. Axelrod, Y. Berkovich, and A. Ioinovici, "Switched-capacitor/switched-inductor structures for getting transformer less hybrid DC–DCPWM converters," IEEE Trans. Circuits Syst. I: Reg. Papers, vol. 55, no. 2, pp. 687–696, Mar. 2008.
[7] Z. Qun and F. C. Lee, "High-efficiency, high step-up DC–DC converters,"IEEE Trans. Power Electron., vol. 18, no. 1, pp. 65–73, Jan. 2003.
[8] H. Yi-Ping, C. Jiann-Fuh, L. Tsorng-Juu, and Y. Lung-Sheng, "A novel high step-up DC–DC converter for a microgrid system," IEEE Trans. Power Electron., vol. 26, no. 4, pp. 1127–1136, Apr. 2011.
[9] L. Wuhua, F. Lingli, Z. Yi, H. Xiangning, X. Dewei, and W. Bin, "High step-up and high-efficiency fuel-cell power-generation system with active clamp flyback-forward converter," IEEE Trans. Ind. Electron., vol. 59,no. 1, pp. 599–610, Jan. 2012.
[10] Y. Changwoo, K. Joongeun, and C. Sewan, "Multiphase DC–DC converters using a boost-half-bridge cell for high-voltage and high-power applications," IEEE Trans. Power Electron., vol. 26, no. 2, pp. 381–388,Feb. 2011.
[11] R. D. Middlebrook, "Transformer less DC-to-DC converters with large conversion ratios," IEEE Trans. Power Electron., vol. 3, no. 4, pp. 484–488, Oct. 1988.
[12] A. A. Fardoun and E. H. Ismail, "Ultra step-up DC–DC converter with reduced switch stress," IEEE Trans. Ind. Appl., vol. 46, no. 5, pp. 2025–2034, Sep./Oct. 2010.
[13] M. Prudente, L. L. Pfitscher, G. Emmendoerfer, E. F. Romaneli, and R. Gules, "Voltage multiplier cells applied to non-isolated DC–DC converters,"IEEE Trans. Power Electron., vol. 23, no. 2, pp. 871–887, Mar.2008.